Int. J. Morphol.,
40(2):407-413, 2022.

Tooth and Pulp Chamber Automatic Segmentation with Artificial Intelligence Network and Morphometry Method in Cone-beam CT

Segmentación Automática de Cámaras Dentales y Pulpares con Red de Inteligencia Artificial y Método de Morfometría en TC de Haz Cónico

Huifang Yang[1,2,3]; Xinwen Wang[2,4] & Gang Li[2,5]

YANG, H.; WANG, X. & LI, G. Tooth and pulp chamber automatic segmentation with Artificial intelligence network and morphometry method in Cone-beam CT. *Int. J. Morphol., 40(2)*:407-413, 2022.

SUMMARY: This study aims to extract teeth and alveolar bone structures in CBCT images automatically, which is a key step in CBCT image analysis in the field of stomatology. In this study, semantic segmentation was used for automatic segmentation. Five marked classes of CBCT images were input for U-net neural network training. Tooth hard tissue (including enamel, dentin, and cementum), dental pulp cavity, cortical bone, cancellous bone, and other tissues were marked manually in each class. The output data were from different regions of interest. The network configuration and training parameters were optimized and adjusted according to the prediction effect. This method can be used to segment teeth and peripheral bone structures using CBCT. The time of the automatic segmentation process for each CBCT was less than 13 min. The Dice of the evaluation reference image was 98 %. The U-net model combined with the watershed method can effectively segment the teeth, pulp cavity, and cortical bone in CBCT images. It can provide morphological information for clinical treatment.

KEY WORDS: Convolutional neural network; Teeth segmentation; Cone-beam computer tomography; Morphology.

INTRODUCTION

Cone-beam computed tomography (CBCT) is widely used in the field of stomatology. It can record abundant information on the maxilla-facial region. With the coordinate information and gray value information, many unexpected details of the disease can be effectively detected. CBCT has been used to assess bone density, bone resorption, and bone augmentation in three dimensions. In dental implants, there are many methods for studying bone repair and reconstruction (Hasan *et al*., 2015). Furthermore, the periodontal state and shape of the tooth root have also attracted increasing attention (Kapila & Nervina, 2015). The application of 3D segmentation and reconstruction technology has gradually been applied to rebuild the anatomical structures of teeth and surrounding tissues.

In orthodontics and periodontics, there are applicable methods to explore the development of bone resorption and recession. Al-Zahrani *et al*. (2017) and Zhang *et al*. (2020) used CBCT data to analyze the progression on of periodontitis disease. For example, the patient's alveolar bone shrinks owing to disease progression, and may cause multiple teeth to move or loosen. Therefore, CBCT can provide information about bone tissue to help doctors detect signs of periodontitis. If the teeth can be segmented accurately, it can be refined to analyze the changes in periodontal disease, such as periodontal ligament and bone resorption of a certain tooth.

In orthodontic treatment, doctors generally use medical image processing software, such as MIMICS (Materialize, Belgium) and AMIRA (Thermo Fisher Scientific, France) to segment teeth. According to the segmentation results, the doctor can create some corresponding clinical programs. The software can realize automatic threshold segmentation based on gray density values, but cannot realize complete tissue

[1] Center of Digital Dentistry, Peking University School and Hospital of Stomatology, Beijing China.
[2] National Center of Stomatology, National Clinical Research Center of Oral Diseases & National Engineering Research Center of Oral Biomaterials and Digital Medical Devices, Beijing, China.
[3] Beijing Key Laboratory of Digital Stomatology & Research Center of Engineering and Technology for Computerized Dentistry Ministry of Health, Beijing China.
[4] Department of Orthodontics, Peking University School and Hospital of Stomatology, Beijing China.
[5] Department of Oral and Maxillofacial Radiology, Peking University School and Hospital of Stomatology, Beijing China.

Received: 2021-10-26 Accepted:2022-01-21

automatic segmentation. Deep learning, a branch of artificial intelligence, has many advantages for analyzing data with speed and precision.

There are three types of tooth segmentation methods: threshold method, active contour model method, and neural network method (Heo *et al*., 2021). The threshold method is based on different gray values between the tooth and the periodontal ligament. The main problem of segmentation is to obtain the optimal threshold; however, the optimal threshold for different samples is different. Therefore, for different samples, the optimal threshold should be re-explored. Heo & Chae (2004) proposed an optimal threshold scheme for segmentation of teeth. However, the tissue near the tooth root is complicated, and it is difficult to distinguish the alveolar bone from the tooth root with a single threshold rang. Akhoondali *et al*. (2009) proposed a fast and automatic segmentation method using a region-growing method. Because the gray values of the cancellous bone and cortical bone near the root are similar, the teeth cannot be segmented automatically. The active contour method is an interactive segmentation method based on contour reconstruction. The contours of the tooth are marked by the shortest diagonal method or level s*et al*gorithm, and the 3D tooth model is reconstructed along the contour of the tooth (Barone *et al*., 2016; Gan *et al*., 2018; Fan *et al*., 2019; Amorim *et al*., 2020). The research on teeth segmentation combining morphology features revealed that the actual measured Root Mean Square (RMS) value is 0.39 mm, less than 0.4 mm (Yang & Wang, 2020).

Lee *et al*. (2020) used a histogram-based method as a preprocessing step to compute the average gray density level of the bone and tooth regions. Simultaneously, they developed a posterior probability function (PPF) with CNN models to improve the segmentation performance. Experimental results showed that the proposed method is better than the existing methods (Lee *et al*.). In addition, Lee *et al*. considered the impact of metal artifacts during segmentation by adjusting the posture distribution of the teeth, marking all the photos of two CBCT samples and five photos of other CBCTs, and then proceeding to the teeth one by one. The results showed that the convolutional neural networks used can reduce the inter-overlapping area between boxes (Chung *et al*., 2020).

Because the Hounsfield unit (HU) values of different CBCT images are inconsistent, different segmentation correction methods are used during segmentation (Pauwels *et al*., 2015). In this study, we used the U-net model to segment CBCT data for dental hard tissue, pulp cavity, cortical bone, and cancellous bone simultaneously. To relieve the overfitting problem as training samples, generative adversarial networks can be applied to medical images (Chen *et al*., 2021).

MATERIAL AND METHOD

Data acquisition and preprocessing. In this study, we used data from the Peking University School of Stomatology, which were scanned with a CBCT machine (DCT Pro; Vatech, Co., Ltd, South Korea). Voxel size was 250*250*250 mm. The data were saved in the Digital Imaging and Communications in Medicine (DICOM) 3.0 format. CBCT manufacturers and software providers present gray scales as the HU (Razi *et al*., 2014). With normalization, the HU value of CBCT data was set to 0-1. TensorFlow (Abadi *et al*., 2016) and Keras (Chollet, 2018) libraries were integrated in the dragonfly software (version 4.3, Objects Research Systems, Montreal, QC, Canada) (Reznikov *et al*., 2020). A computer with an Intel® Xeon W-2145 E5 CPU, an NVIDIA Quadro P4000 (8GB) graphics card, and 64GB RAM was used.

Normalization. To reduce the amount of calculated data, preprocessing should be performed. First, the data were normalized. In CBCT, the images are presented with HU (Pauwels *et al*.). HU is a dimensionless unit universally used in computed tomography (CT) scanning to express CT numbers obtained from a linear transformation of the measured attenuation coefficients (Hounsfield, 1980). The results are based on arbitrarily assigned densities of air and pure water. It is in a scale running from -1000 HU for air and over 3000 for metals (Glide-Hurst *et al*., 2013). In this research, normalization was performed by a linear function:

$$y = mx + b$$

where x refers to the HU obtained from the CBCT machine, with a minimum value (-1000) and a maximum value (3000-20000), which was dependent on different machine and scan parameters and radiation dose; y is the set HU value in the range of 0-1. In these data, the average HU value was 0.16. The value of the standard deviation was 0.15. The probability distribution map of a sample's CBCT HU is shown in Figure 1, and after normalization, the probability distribution map of HU is shown in Figure 2.

Data annotation. The goal of semantic image segmentation is to label each pixel of an image with a corresponding class of representation. The output itself is a high-resolution image (typically of the same size as the input image) in which each pixel is classified into a particular class. Every image was marked with five different colors that were used to represent five classes (teeth, pulp chamber, cortical bone, trabecular bone, and background). The images were normalized, as shown by the left image in Figure 3, and the manually marked result is presented by the right image in Figure 3. The image was divided into five classes, where the teeth were green,

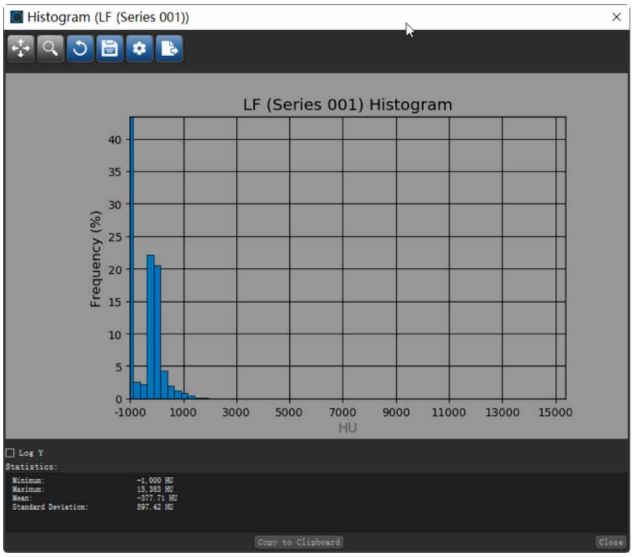

Fig. 1. Probability distribution map of a sample's CBCT HU.

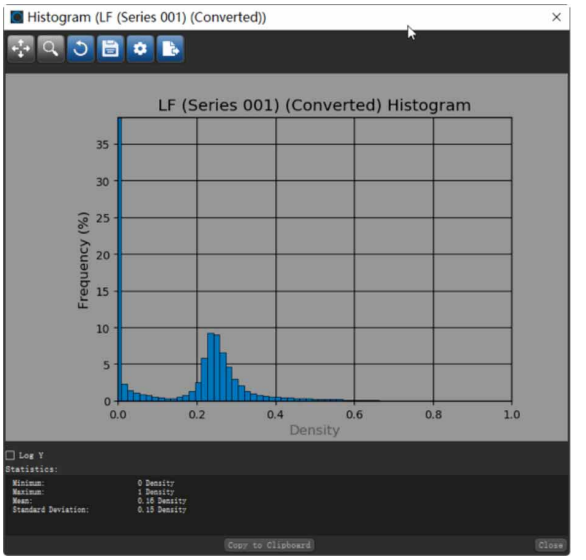

Fig. 2. Probability distribution map of HU value after CBCT image normalization.

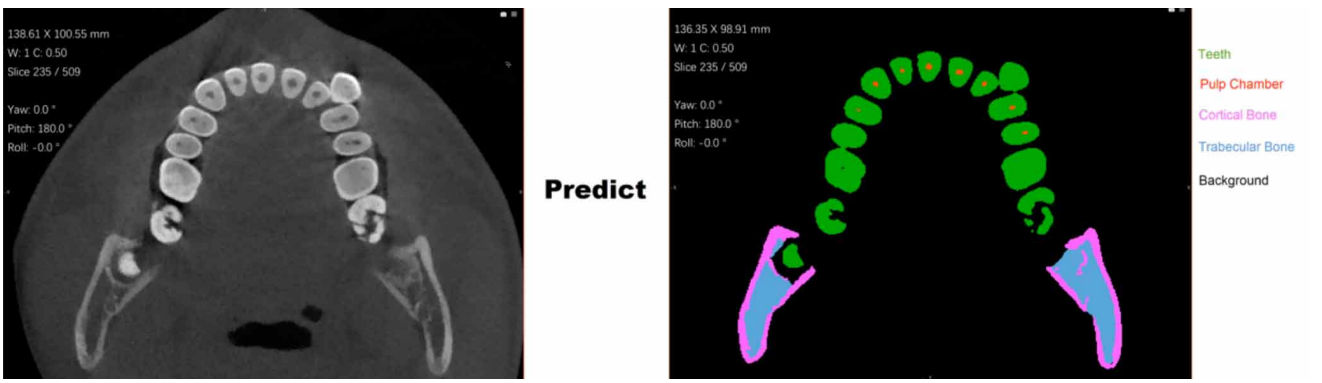

Fig. 3. Semantic segmentation of the CBCT. The original image is normalized, as shown by the left picture, and the manually marked result is presented by the right picture. The image is divided into five classes, in which the teeth are green, the pulp chamber is red, the cortical bone is pink, the trabecular bone is blue, and the background is black.

pulp chamber was red, cortical bone was pink, trabecular bone was blue, and background was black. The images were annotated in the transverse plane, as shown in Figure 4. The operator can annotate different regions of interest (ROIs) using the local Otsu, Atlas, or threshold segmentation method. Five images after annotation are shown in Figure 5 in the transverse direction of the CBCT.

Data augmentation. Data augmentation is a method for artificially generating more training samples to increase the diversity of the training data. This can be achieved by applying affine transformations (e.g., rotation and scaling), flipping vertically and horizontally to the original labeled samples. The brightness of the image was randomly changed by providing a brightness factor because of the different HU values of different CBCT data. The brightness factor was chosen randomly in the range [-0.2, 2]. The change in brightness allows a model to generalize across images trained

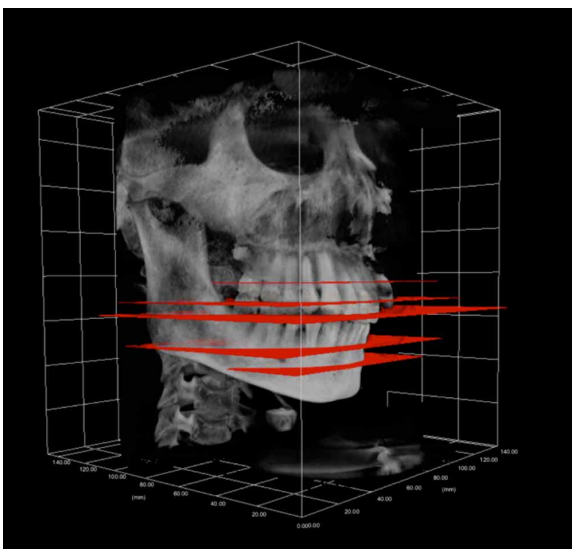

Fig. 4. Image selected from transverse plane.

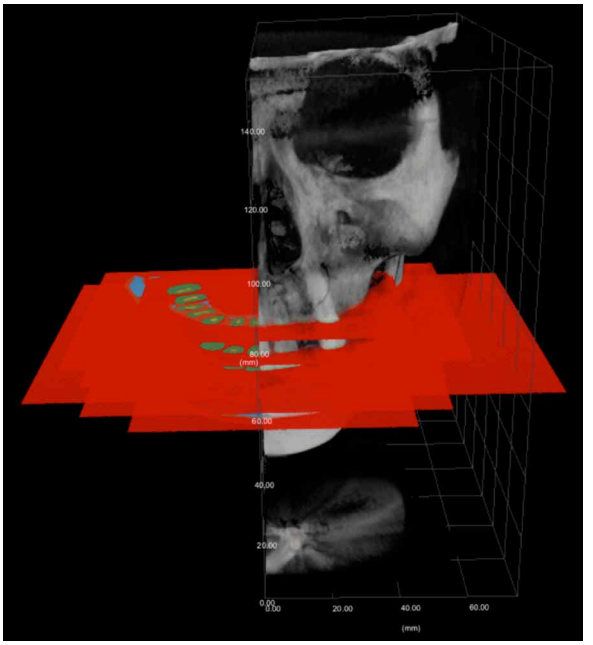

Fig. 5. Annotated result of one CBCT samples

on different illumination levels. The data were augmented 10 times using different factors. An example of data augmentation is shown in Figure 6.

Fig. 6. Data augmentation example.

Semantic image segmentation with U-net. The goal of this step is to label each pixel of an image with a corresponding class. The 2D U-net model consists of an encoder and a decoder part (Ronneberger *et al*., 2015). The training parameters in the U-net are as follows: the number of layers in the model = 4, Patch size = 64, Batch size = 32, and Loss function = Dice loss. The training is conducted with 100 epochs, however, it stops if there is no improvement in 'value loss' for 10 consecutive epochs. The overall network structure is illustrated in Figure 7. The set was partitioned into learning and validation subsets (80 % and 20 %, respectively). After the training, we previewed the results of applying a deep learning model to a selected dataset. Thereafter, we applied the model to the whole slices of CBCT and obtained a multi-ROI.

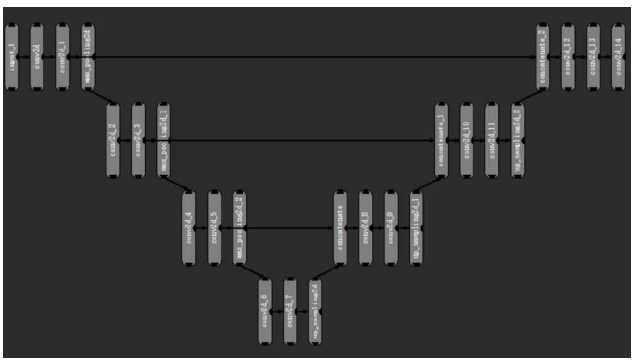

Fig. 7. 2D U-net architecture.

We removed image noise from the ROIs, smoothed the data, and created a 3D model reconstruction from the ROIs. Small disconnected noises that were less than 0.8 nm^3 were excluded. Thereafter, the final ROI was converted into a 'mesh' data.

Individual tooth segmentation -Watershed method to segment each tooth. Marker-controlled watershed transform (WMT) was adopted to segment individual tooth (Chen *et al*., 2020). A different class of models, known as instance segmentation models, which distinguishes between separate objects of the same class, was adopted to segment individual teeth. We set the pulp as the marker and used the distance map of the teeth (the union of Class 1 and Class 5) as a landscape. Thereafter, watershed segmentation was performed to obtain the individual tooth.

RESULTS

This study used deep learning methods to automatically segment and extract teeth and surrounding tissues in CBCT images. The input data for neural network training were CBCT images and five marked classes, and the output data were multi-ROI. A 2D U-net neural network model was adopted. The parameters were optimized and adjusted according to the prediction effect. Neural network training, image segmentation, and reconstruction were completed using Dragonfly software. This method can segment teeth and peripheral regions in CBCT. After training, the CBCT image sequence was segmented automatically. The Dice score (DSC) of the valuation data (20 % pixels in the marked images) was 98.59 %.

TP is true positive, *TN* is true negative, *FP* is false positive, and *FN* is false negative.

$$DSC = 2TP/(2TP + FP + FN)$$

By optimizing the parameters step by step and modifying the annotation data, the optimal segmentation result can be obtained. The network trained for 100 epochs took 4 h and 15 min, while for 21 epochs took 55 min and 3 s. Using the normalized CBCT data as the test set, all segmentation with the trained model took 12 min and 20 s. The segmented results are presented in Figure 8. The U-net model of Dragonfly software can effectively segment the teeth, pulp cavity, cancellous bone, and cortical bone in the CBCT image. Furthermore, it can provide morphological information for clinical treatment (Figs. 9 to 11).

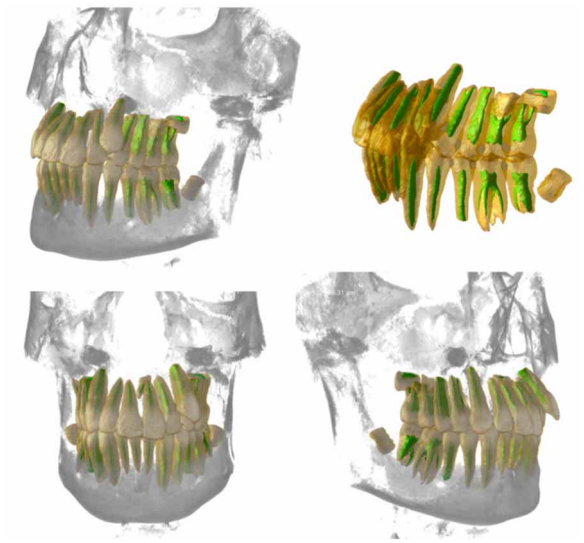

Fig. 8. Result after the semantic segmentation (in the picture, the green data are pulp chamber, and the yellow data are teeth).

Fig. 9. Result after the semantic segmentation (in the picture, the pink data are bones)-

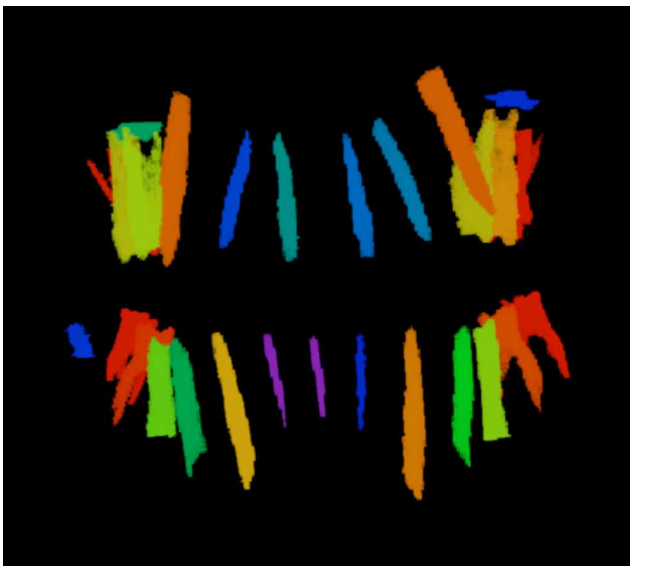

Fig. 10. 3D view of dental pulp chamber.

Fig. 11. Teeth after segmentation.

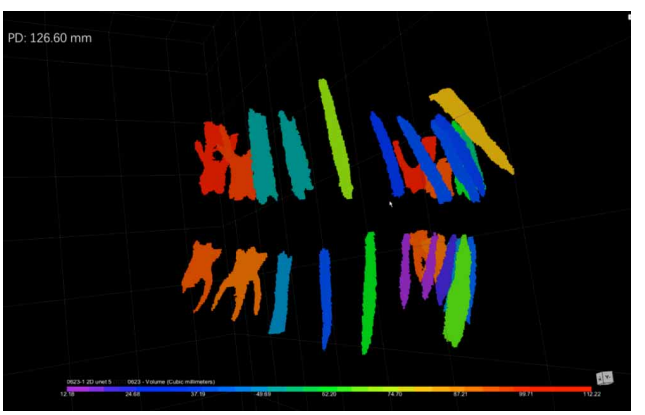

Fig. 12. 3D side view of dental pulp chamber.

DISCUSSION

The quality of tooth segmentation determines the accuracy of treatment in orthodontic and periodontitis treatment planning. In this study, we proposed an automated tooth and bone segmentation method for CBCT.

Lee *et al*. segmented teeth by marking all the photos of two CBCT samples and five photos of other CBCTs to train a convolutional neural network (Chung *et al*.). In this study, we realized semi-automatic or automatic labeling of multi-dimensional data based on five photos of CBCT samples with U-net and data augmentation methods. To evaluate the performance of the model, we used data from the Peking University School of Stomatology to show that the proposed model can segment the whole CBCT data to several ROIs in other data.

Normalization is important for image preprocessing. If the image is not preprocessed, the network will diverge during the training process, resulting in the loss function value reaching infinity. Normalization is performed by a linear change, and the resulting value is between 0 and 1. If the normalized range is different, the result will be affected. However, with data augmentation in the training process, the trained U-net model can be used in a new CBCT.

Gan *et al*. proposed a method to extract the connected region of the tooth and alveolar bone from CT images using a global convex level set model. However, the method can only be used in subjects whose teeth are in an open bite position. In this study, we proposed a U-net combined with a data augmentation method to achieve automatic segmentation of different tissues in a closed bite.

Lahoud *et al*. (2021) used the AI algorithm to segment teeth in CBCT; however, it has some limitations, such as the network can only be used in premolars, but not in molars. Furthermore, it segments one or more teeth; thus, in different tooth segmentations, corresponding errors will occur. In addition to tooth segmentation, we segmented the pulp chamber (Fig. 12) and bones, which will provide more morphometric information for oral surgery, orthodontics, or guided endodontics.

CONCLUSION

In this study, training the network by manually labeling five pictures significantly improves the efficiency of image segmentation. In the future, by expanding the amount of data, a fully automatic segmentation and identification of multiple tissues in the oral cavity can be performed. It can provide morphological guidance for orthodontics, implants, and periodontal diseases. The accuracy of the automatic segmentation can be improved, which will greatly improve the automated diagnostics in dentistry.

ACKNOWLEDGEMENTS. This work is supported by PKU-Baidu Fund(2020BD037).

YANG, H.; WANG, X. & LI, G. Segmentación automática de cámaras dentales y pulpares con red de inteligencia artificial y método de morfometría en TC de haz cónico. *Int. J. Morphol., 40(2)*:407-413, 2022.

RESUMEN: El objetivo del presente estudio fue extraer estructuras dentarias y óseas alveolares desde imágenes CBCT automáticamente, lo cual es un paso clave en el análisis de imágenes CBCT en el campo de la estomatología. En este estudio, se utilizó la segmentación de tipo emántica para la segmentación automática. Se ingresaron cinco clases de imágenes CBCT marcadas, para el entrenamiento de la red neuronal U-net. El tejido duro del diente (incluidos esmalte, dentina y cemento), la cavidad de la pulpa dentaria, hueso cortical, hueso esponjoso y otros tejidos se marcaron manualmente en cada clase. Los datos se obtuvieron de diferentes regiones de interés. La configuración de la red y los parámetros de entrenamiento se optimizaron y ajustaron de acuerdo con un análisis predictivo. Este método se puede utilizar para segmentar dientes y estructuras óseas periféricas mediante CBCT. El tiempo del proceso de segmentación automática para cada CBCT fue menor a 13 min. El "Dice" de evaluación de la imagen de referencia fue de 98 %. El modelo U-net combinado con el método "watershed"puede segmentar eficazmente los dientes, la cavidad pulpar y el hueso cortical en imágenes CBCT. Puede proporcionar información morfológica para el tratamiento clínico.

PALABRAS CLAVE: Red neuronal convolucional; Segmentación de dientes; Tomografía computarizada de haz cónico; Morfología.

REFERENCES

Abadi, M.; Barham, P.; Chen, J.; Chen, Z.; Davis, A.; Dean, J.; Devin, M.; Ghemawat, S.; Irving, G.; Isard, M.; *et al*., *TensorFlow: A System for Large-Scale Machine Learning. Savannah, Proceedings of Osdi'16*: 12th Usenix Symposium on Operating Systems Design and Implementation, 2016. pp.265-83.

Akhoondali, H.; Zoroofi, R. A. & Shirani, G. Rapid automatic segmentation and visualization of teeth in CT-scan data. *J. Appl. Sci., 9(11)*:2031-44, 2009.

Al-Zahrani, M. S.; Elfirt, E. Y.; Al-Ahmari, M. M.; Yamany, I. A.; Alabdulkarim, M. A. & Zawawi, K. H. Comparison of cone beam computed tomography-derived alveolar bone density between subjects with and without aggressive periodontitis. *J. Clin. Diagn. Res., 11(1)*:ZC118-ZC121, 2017.

Amorim, P. H. J.; Moraes, T. F.; Silva, J. V. L.; Pedrini, H. & Ruben, R. B. Reconstruction of panoramic dental images through bezier function optimization. *Front. Bioeng. Biotechnol., 8*:794, 2020.

Barone, S.; Paoli, A. & Razionale, A. V. CT segmentation of dental shapes by anatomy-driven reformation imaging and B-spline modelling. *Int. J. Numer Method Biomed. Eng., 32(6)*, 2016. DOI: https://www.doi.org/10.1002/cnm.2747

Chen, X.; Li, Y.; Yao, L.; Adeli, E. & Zhang, Y. Generative adversarial U-Net for domain-free medical image augmentation. *ArXiv, 2101*.04793, 2021.

Chen, Y.; Du, H.; Yun, Z.; Yang, S.; Dai, Z.; Zhong, L.; Feng, Q. & Yang, W. Automatic segmentation of individual tooth in dental CBCT images from tooth surface map by a Multi-Task FCN. *IEEE Access, 8*:97296-309, 2020.

Chollet, F. *Keras: The Python Deep Learning library.* Astrophysics Source Code Library, 2018.

Chung, M.; Lee, M.; Hong, J.; Park, S.; Lee, J.; Lee, J.; Lee, J. & Shin, Y. G. Pose-aware instance segmentation framework from cone beam CT images for tooth segmentation. *Comput. Biol. Med., 120*:103720, 2020.

Fan, Y.; Beare, R.; Matthews, H.; Schneider, P.; Kilpatrick, N.; Clement, J.; Claes, P.; Penington, A. & Adamson, C. Marker-based watershed transform method for fully automatic mandibular segmentation from CBCT images. *Dentomaxillofac Radiol., 48(2)*:20180261, 2019.

Gan, Y.; Xia, Z.; Xiong, J.; Li, G. & Zhao, Q. Tooth and alveolar bone segmentation from dental computed tomography images. *IEEE J. Biomed. Health Inform., 22(1)*:196-204, 2018.

Glide-Hurst, C.; Chen, D.; Zhong, H. & Chetty, I. J. Changes realized from extended bit-depth and metal artifact reduction in CT. *Med. Phys., 40(6)*:061711, 2013.

Hasan, I.; Dominiak, M.; Blaszczyszyn, A.; Bourauel, C.; Gedrange, T. & Heinemann, F. Radiographic evaluation of bone density around immediately loaded implants. *Ann. Anat., 199*:52-7, 2015.

Heo, H. & Chae, O. S. Segmentation of tooth in CT images for the 3D reconstruction of teeth. *SPIE*, 5298, 2004. DOI: https://www.doir.org/10.1117/12.526111

Heo, M. S.; Kim, J. E.; Hwang, J. J.; Han, S. S.; Kim, J. S.; Yi, W. J. & Park, I. W. Artificial intelligence in oral and maxillofacial radiology: what is currently possible? Dentomaxillofac. *Radiol., 50(3)*:20200375, 2021.

Hounsfield, G. N. Computed medical imaging. Nobel lecture, Decemberr 8, 1979. *J. Comput. Assist. Tomogr., 4(5)*:665-74, 1980.

Kapila, S. D. & Nervina, J. M. CBCT in orthodontics: assessment of treatment outcomes and indications for its use. *Dentomaxillofac. Radiol., 44(1)*:20140282, 2015.

Lahoud, P.; EzEldeen, M.; Beznik, T.; Willems, H.; Leite, A.; Van Gerven, A. & Jacobs, R. Artificial intelligence for fast and accurate 3-dimensional tooth segmentation on cone-beam computed tomography. *J. Endod., 47(5)*:827-35, 2021.

Lee, S.; Woo, S.; Yu, J.; Seo, J.; Lee, J. & Lee, C. Automated CNN-Based Tooth Segmentation in Cone-Beam CT for Dental Implant Planning. *IEEE Access, 8*:50507-18, 2020.

Pauwels, R.; Jacobs, R.; Singer, S. R. & Mupparapu, M. CBCT-based bone quality assessment: are Hounsfield units applicable? *Dentomaxillofac. Radiol., 44(1)*:20140238, 2015.

Razi, T.; Niknami, M. & Ghazani, F. A. Relationship between Hounsfield Unit in CT Scan and Gray Scale in CBCT. *J. Dent. Res. Dent. Clin. Dent. Prospects, 8(2)*:107-10, 2014.

Reznikov, N.; Buss, D. J.; Provencher, B.; McKee, M. D. & Piché, N. Deep learning for 3D imaging and image analysis in biomineralization research. *J. Struct. Biol., 212(1)*:107598, 2020.

Ronneberger, O.; Fischer, P. & Brox, T. U-Net: Convolutional Networks for Biomedical Image Segmentation. *arXiv*:1505.04597v1, 2015.

Yang, H. & Wang, S. Research on a segmentation and evaluation method combining tooth morphology features. *Int. J. Morphol., 38(5)*:1325-9, 2020.

Zhang, X.; Li, Y.; Ge, Z.; Zhao, H.; Miao, L. & Pan, Y. The dimension and morphology of alveolar bone at maxillary anterior teeth in periodontitis: a retrospective analysis-using CBCT. *Int. J. Oral Sci., 12(1)*:4, 2020.

Corrresponding author:
Huifang Yang
No. 22 South Street
Zhongguancun Haidian District
Beijing, 100081
PR CHINA

E-mail: yanghuifang@pkuss.edu.com.cn